Journal of Inorganic Biochemistry 239 (2023) 112089

Contents lists available at ScienceDirect

Journal of Inorganic Biochemistry

journal homepage: www.elsevier.com/locate/jinorgbio

Relaxation-based NMR assignment: Spotlights on ligand binding sites in human CISD3

Deborah Grifagni [a,b], José M. Silva [a], Francesca Cantini [a,b], Mario Piccioli [a,b,*], Lucia Banci [a,b,*]

[a] Magnetic Resonance Center and Department of Chemistry, University of Florence, Via L. Sacconi 6, 50019 Sesto Fiorentino, Italy
[b] Consorzio Interuniversitario Risonanze Magnetiche Metallo Proteine, Via L. Sacconi 6, 50019 Sesto Fiorentino, Italy

ARTICLE INFO

Keywords:
Iron-Sulfur
NEET proteins
CISD3
Miner 2
cancer
Paramagnetic relaxation enhancement

ABSTRACT

CISD3 is a mitochondrial protein belonging to the NEET proteins family, bearing two [Fe_2S_2] clusters coordinated by CDGSH domains. At variance with the other proteins of the NEET family, very little is known about its structure-function relationships. NMR is the only technique to obtain information at the atomic level in solution on the residues involved in intermolecular interactions; however, in paramagnetic proteins this is limited by the broadening of signals of residues around the paramagnetic center. Tailored experiments can revive signals of the cluster surrounding; however, signals identification without specific residue assignment remains useless. Here, we show how paramagnetic relaxation can drive the signal assignment of residues in the proximity of the paramagnetic center(s). This allowed us to identify the potential key players of the biological function of the CISD3 protein.

1. Introduction

The complete NMR resonance assignment of a biological macromolecule is mandatory to monitor site-specific interactions with drugs and/or with other biomolecules in solution. These interactions could produce very small chemical shift perturbations localized on specific residues; therefore, the complete NMR assignment is needed to obtain atom-level information. In metalloproteins, the metal centers usually play a pivotal role in the protein function/structure; together with their ligands, they are expected to be the main target for ligands and protein interactions [1–4]. Furthermore, also electrostatic charges, hydrogen bond networks, and hydrophobic/hydrophilic pockets around the metal site are frequently involved in protein-ligand interactions [5]. Consequently, also residues in the proximity of the metal center, but not directly involved in its coordination, play a crucial role. In paramagnetic metalloproteins, nuclear spin relaxation rates are enhanced by contributions arising from the hyperfine interactions between electron and nuclear spins. As a consequence, nuclear spins close to a paramagnetic center relax too fast for obtaining NMR spectra suitable for an extensive assignment and, often, even for detecting them [6]. Iron-sulfur proteins offer many interesting case studies to address the feasibility of an extended NMR assignment in the presence of paramagnetic centers [7,8] and to exploit the paramagnetic relaxation enhancements as a source structural constraints [9–11].

Discovered about 15 years ago, NEET proteins climbed the "top of the pop" of metalloproteins due to their possible role in ROS and iron homeostasis regulations [12–14]. They are overexpressed in a variety of cancer types and are potential targets for diabetes treatment [15,16]. All NEET proteins share a 39 amino acid sequence, called CDGSH domain, which contains a 3Cys:1His motif, able to bind a [Fe_2S_2] cluster cofactor [17]. The CDGSH domain contains a β-cap region, the conserved consensus sequence responsible for the binding of the cluster: C-X-C-X2-(S/T)-X3-P-X-CAG-(S/A/T)-H [18] and a α-helix encompassing part of the consensus sequence and the C-term end of the domain. CISD3 (also known as MiNT or Miner-2) is a matrix mitochondrial protein of 127 amino acids able to coordinate two [Fe_2S_2] clusters. The NEET protein family is completed with mitoNEET and NAF-1 [19]. At variance with the other human NEET proteins, CISD3 contains two CDGSH cluster-binding motifs within a single polypeptide chain that folds as a monomer in solution [17,20].

Crystal structure of the CISD3 mutant (H75C, H113C) [PDB ID code 6AVJ] showed that the protein exhibits a pseudo-symmetrical fold that provides a hydrophobic region on one side and a relatively hydrophilic surface on the diametrically opposed surface [20]. The presence of two

* Corresponding authors at: Magnetic Resonance Center and Department of Chemistry, University of Florence, Via L. Sacconi 6, 50019 Sesto Fiorentino, Italy.
E-mail addresses: grifagni@cerm.unifi.it (D. Grifagni), silva@cerm.unifi.it (J.M. Silva), cantini@cerm.unifi.it (F. Cantini), piccioli@cerm.unifi.it (M. Piccioli), banci@cerm.unifi.it (L. Banci).

https://doi.org/10.1016/j.jinorgbio.2022.112089
Received 31 August 2022; Received in revised form 26 November 2022; Accepted 1 December 2022
Available online 5 December 2022

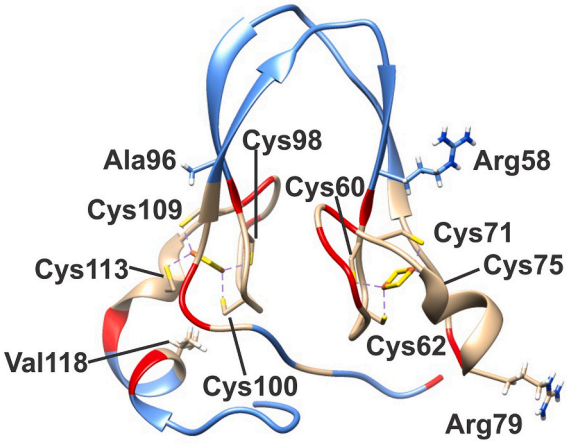

Fig. 1. Structure of the H75C and H113C mutant CISD3 (PDB: 6AVJ) [20]. In cyan are the assigned diamagnetic amide resonances using standard triple resonance approach; in red are the assigned paramagnetic amide resonances using the relaxation-based NMR assignment. In kaki are the not assigned residues. The $[Fe_2S_2]$ clusters, the iron ligands and residues mentioned in the text, numbered according to CISD3 sequence (P0C7P0), are in sticks. (For interpretation of the references to colour in this figure legend, the reader is referred to the web version of this article.)

CDGSH domains in the same polypeptide chain has been proposed as the ancient archetype of the CDGSH proteins [21]. The soluble 93 aa construct, spanning from residue 37 to residue 127, contains two CDGSH domains and, compared to the other NEET proteins, is the smallest sequence able to bind two $[Fe_2S_2]$ clusters by the 3Cys:1His motif. In contrast to mitoNEET and NAF-1, very little is known about the function of human CISD3. Previous studies showed that knockdown of CISD3 leads to increased accumulation of mitochondrial labile iron, as well as increased mitochondrial reactive oxygen production [20]. It has been also proposed that CISD3 is involved in mitochondrial functions and morphology [22,23]. A recent study presented evidence that depletion of CISD3 leads to an increase of ferroptosis of tumor cells previously treated with erastin [24]. Under the stimulating hypothesis that CISD3 is a target for anticancer therapies, an extensive NMR assignment of the protein would be mandatory to monitor at the molecular level the interactions of this protein with other protein partners and/or ligands. Within this frame, we expressed and purified the 93 aa construct of wild type CISD3 in *E. coli*. The protocol for protein expression and purification and the NMR experiments acquired on $^{13}C/^{15}N$ labelled CISD3 in its reduced $2[Fe_2S_2]^{+}$ form are reported in the Materials and Methods section.

2. Results

The NMR assignment of CISD3 is extremely challenging, because we expect that most of the protein would be affected by the paramagnetic clusters [25]. However, the crystal structure of the (H75C, H113C)

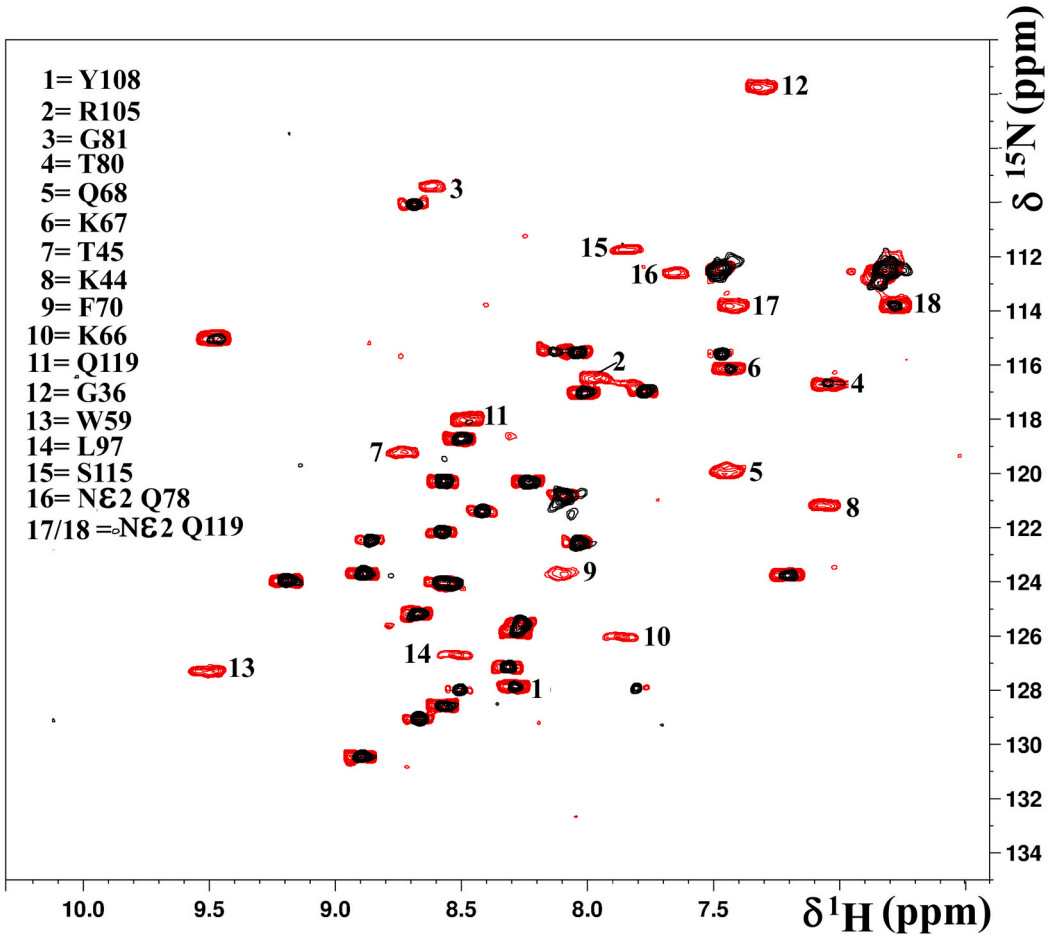

Fig. 2. Overlay of standard ^{15}N HSQC (black) vs ^{15}N HSQC-AP (red). The latter has been collected with INEPT and recycle delays of 0.7 ms and 150 ms, respectively. Experiments were performed at 500 MHz at 298 K. The buffer was 50 mM phosphate buffer, 150 mM NaCl, pH 7.5. The sample concentration was 0.5 mM. (For interpretation of the references to colour in this figure legend, the reader is referred to the web version of this article.)

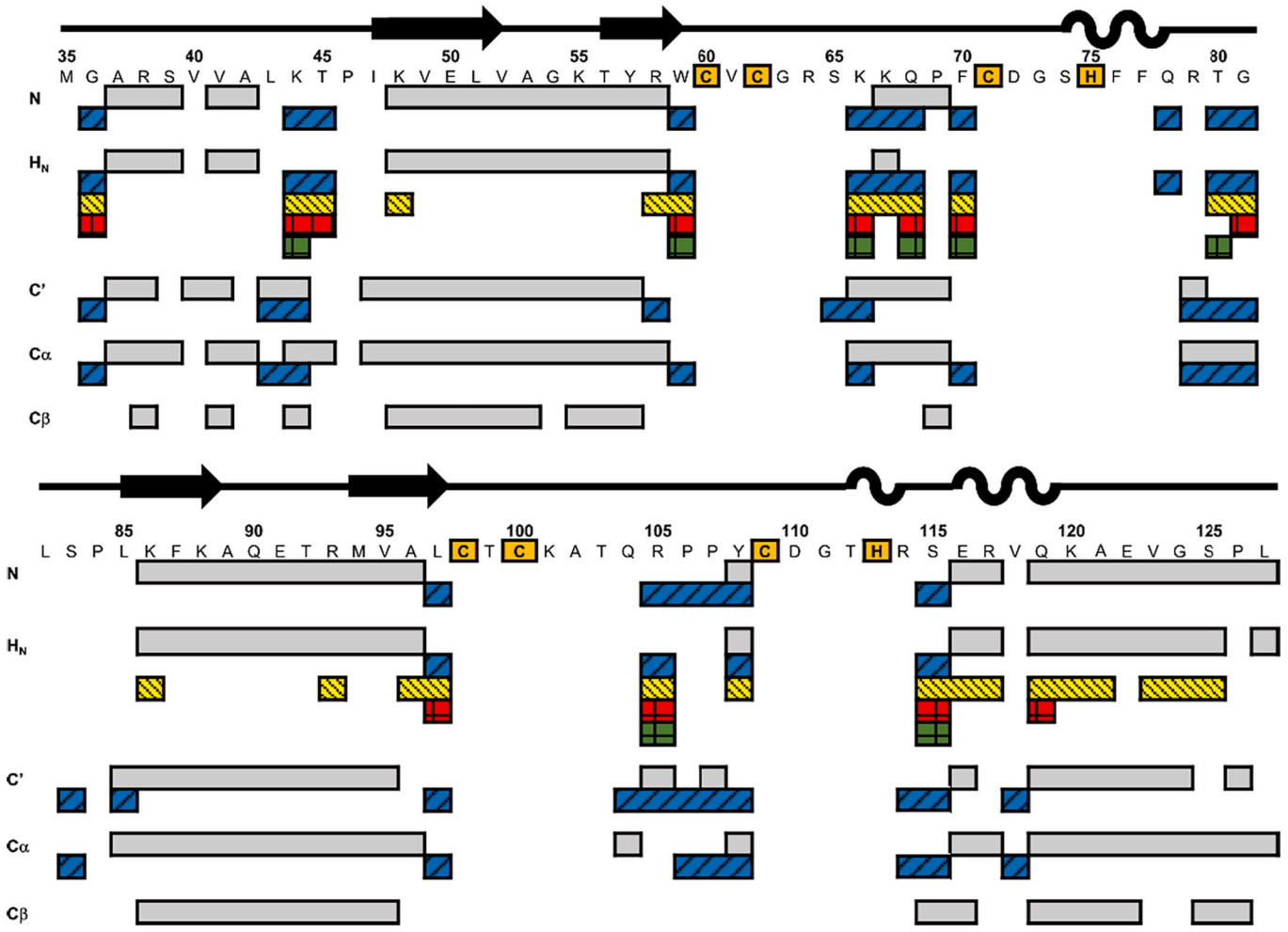

Fig. 3. Summary of sequential connectivities and assignments obtained with conventional triple resonance experiments (gray), paramagnetic tailored experiments (blue) and paramagnetic relaxation enhancement. For the paramagnetic tailored experiments, the blue colored bar reports only those connectivities that have been used to extend the backbone assignment obtained via conventional triple resonance experiments. HN residues that were used to obtain PRE distances are shown in yellow; NH groups that escaped detection in conventional HSQC and that have been recovered only in HSQC-AP experiments are shown in red; HN groups that were assigned thanks to PRE distances are coded in green. Conventional triple resonance experiments that have been used are: HSQC, HNCO, HNCA, HNCOCA, CBCA-CONH, C_CON, C_CACO. Paramagnetic tailored experiments are: HSQC-AP, C_CON, C_CACO-AP. Secondary structure elements are also shown. (For interpretation of the references to colour in this figure legend, the reader is referred to the web version of this article.)

protein variant can be taken as a reliable model to guide the NMR assignment, although we identified some structural differences around His 75 and His 113. With a standard set of triple resonance experiments, the sequence specific assignment of the long 48–58, 86–96, 120–127 stretches and of the shorter 37–39, 41–42 and 116–117 segments was obtained, as shown in Fig. 1. Overall, 37 HN signals out of 87 non-proline residues (40%) are observed in the standard NMR experiments (Fig. S1 of the Supplementary Information). For these residues, all backbone atoms were assigned. According to the crystal structure, the detectable H_N protons with the shortest metal-to-proton distances are Arg 58 and Ala 96 H_N, that are 8.9 Å apart from the closest iron ion. Each of them are located at the end of the β-cap regions, two residues before the first cluster binding Cys (i.e. Cys 60 and Cys 98) in each of the two CDGSH domains. With the single exception of Ala 42, which has been assigned using standard triple resonance experiments even if its HN is only 7.6 Å from the closest metal, a metal-to-proton distance of 8.8 Å sets the threshold for signal detectability: only above that distance the standard assignment procedure can be successfully performed. There are only two residues that escaped detection in the standard NMR experiments, even if they are beyond the 8.8 Å threshold: Arg 79 and Val 118 which, in the X-ray structure, are respectively 9.0 and 9.2 Å apart from the closest iron ion (Fig. 1). Both these residues are located in the α-helices at the C-term of the two CDGSH domains, 4/5 residues apart from the mutated cluster binding histidines (His 75 and His 113). Their undetectability is therefore indicative of the structural differences of the α-helices regions in the WT protein with respect to the Cys-to-His mutant.

NMR is the only tool to monitor ligand binding sites in solution at the atomic level. In order to apply it to the CISD3 case, it is mandatory to extend the assignment to further residues around the [Fe_2S_2] clusters. To this end, we recorded a set of tailored experiments in which acquisition, recycle and coherence transfer delays were optimized to maximize the intensities of signals affected by paramagnetic relaxation, at expenses of spectral resolution and signal-to-noise ratio of slow relaxing signals [26–29].

First a ^{15}N- HSQC-AP experiment allowed us to identify 18 HN resonances (Fig. 2) that in standard ^{15}N-HSQC experiments were missing, or observed as barely detectable peaks, and to measure their relaxation rates. A similar behavior has been observed in the paramagnetic CACO and CON spectra (Table S1), in which additional 25 and 16 signals respectively were observed (Fig. S2).

Subsequently, we measured R_1 and R_2 H_N relaxation rates (Table S2) through a combination of experiments selected and tuned according to the different paramagnetic contributions [27]. As paramagnetic

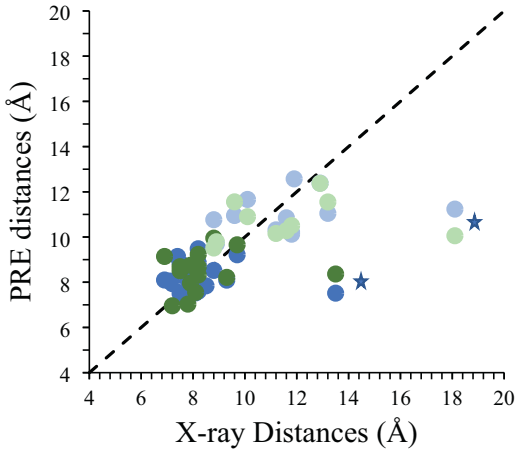

Fig. 4. X-ray vs PRE distances for CISD3 residues with $R_1 > 5\ s^{-1}$. R_1 and R_2 derived distances are shown in blue and green, respectively. Pale colors represent residues located at 9 Å or further from the closest iron. Gly 36 and Arg 93 are marked with stars. (For interpretation of the references to colour in this figure legend, the reader is referred to the web version of this article.)

relaxation rates due to dipolar coupling between nuclear and electron spins are dependent on the inverse sixth power of the metal-to-nucleus distances [30], they can validate or exclude possible assignments arising from paramagnetic experiments and to identify, when multiple assignments are possible, those in agreement with the R_1 and R_2 values. As graphically summarized [31,32] in Fig. 3, paramagnetic tailored experiments helped to extend the stretches that were assigned with the conventional triple resonance assignment. Moreover, some stretches, such as residues 44–45, 80–81 and 104–106, have been identified only in paramagnetic tailored experiments. For these residues, paramagnetic relaxation rates have been crucial to propose their assignment.

Considering diamagnetic contributions to R_1 and R_2 of 2.11 s^{-1} and 36.6 s^{-1} respectively and a τ_c of 5.3×10^{-9} s, as obtained from ^{15}N relaxation experiments (Fig. S3), the data of Table S2 can be converted into metal-to-proton distances, as described in Supplementary Material. We obtained a good agreement between Fe—H distances taken from the crystal structure of the (H75C, H113C) mutant and those obtained from R_1 and R_2 values. This is shown in Fig. 4 for all peaks experiencing R_1 rates >5 s^{-1}.

Relaxation rates obtained using standard experiments [33] and due to signals located at 9 Å or further from the closest iron of the cluster, are shown in pale blue/green in Fig. 4. Residues assigned using experiments tailored to paramagnetic systems (dark blue and dark green,) are located in an annulus between 7 Å and 9 Å away from the closest iron ion of the cluster. The detection and assignment of these signals resulted in reducing the size of the NMR-blind region around both Fe—S clusters, from 9 Å to 7 Å, as shown in Fig. 1, in which residues assigned with the conventional triple resonance approach and with the aid of relaxation measurements are colour-coded in cyan and red, respectively. The good match shown in Fig. 4 between PRE and X-ray distances is a proof of principle that PRE-derived distances can be used to support and confirm the assignment of signals belonging to residues that are close to the paramagnetic center. R_1 and R_2 values provided two independent measurements of the metal-to proton distances, therefore they were used to obtain, for each H_N proton, two distance values which, within the uncertainties, can be taken as upper and lower limit values and are instrumental to the use of relaxation rates for signal assignment. These values are reported in Table S2, last column. There are two residues that significantly deviate from the fitting shown in Fig. 4: Gly 36 and Arg 93, located at 13 Å and 18 Å respectively from the closest iron ion in the crystal structure. Gly 36 is in the N-terminus region, it is therefore likely that there is some structural rearrangement with respect to the crystal structure. Actually, the crystallographic structure has been solved for a protein construct that contains Pro 36. In our construct to facilitate the expression in *E.coli*, Pro 36 has been mutated to Gly 36, and a reorientation of the N-term region with respect to the crystallographic structure is likely to occur. The situation is different for Arg 93, which is at the edge of the β-cap and it is one the residues that are more far apart from the metal ions. None of its neighbor aminoacids shows a relaxation rate enhancement; therefore, we safely exclude the hypothesis of a major structural rearrangement. The occurrence of flexibility or of a local exchange might provide additional contributions to relaxation and account for the observed behavior. Therefore, both Gly 36 and Arg 93 were excluded from further analysis. Overall, the relaxation rates analysis combined with the analysis of paramagnetic ^{15}N- HSQC-AP, CACO and CON spectra, allowed us to assign all the 18 new signals present in the ^{15}N-HSQC-AP experiment thus extending the assignment of amide signals from 40% to 60% and the assignment of Cα and CO signals from 47% to 70%. The signal assignment and the relaxation rate analysis are detailed in the Supplementary Material and in Figs. S4 and S5. The backbone assignment has been deposited in the Biological Magnetic Resonance Data Bank (http://www.bmrb.wisc.edu) under the accession number 51439.

3. Discussion

The use of paramagnetic relaxation enhancement for protein structure determination is well documented [6,28,34–41]. Since decades, methods are being developed to circumvent the loss of the NMR information in paramagnetic systems, because electron relaxation affects the efficiency of coherent and incoherent magnetization transfer among nuclear spins [6,10,28,42–44]. When chemical shift and relaxation rates, affected by the different terms of the hyperfine interaction, are measured and quantified, paramagnetism-based NMR restraints, may replace or complement NOE and scalar coupling restraints for structure calculations [9]. Here, we are making a significant step ahead and show how paramagnetic relaxation rates can be used, together with tailored ^{15}N- HSQC-AP, C_CACO-AP and C_CON experiments, to increase the assignment in the proximity of the active center of a metalloprotein, either native or exogenous. Extending the NMR assignment around the $[Fe_2S_2]$ clusters is particularly relevant, in view of the expected interaction of the NEET proteins with small molecules [16,45,46] or with other protein partners [13,25,47,48].

The approach presented here opens the possibility to experimentally map by NMR the interaction of CISD3 with putative protein partners and ligands. Recently, it has been proposed that CISD3 is involved in the interaction with the voltage-dependent anion channel 1 (VDAC1) and into the cluster transfer to the outer mitochondrial membrane protein mitoNEET [22]. These proposed interactions highlight three possible binding sites involving residues near the paramagnetic center of CISD3 as well as residues belonging to the solvent exposed β-cap region. The interaction of NEET proteins with ligands has been studied in silico for mitoNEET and type-II diabetes approved drugs [49]. The main predicted interactions involved the mitoNEET residues His 48, Ile 49, Gln 50, Arg 76, Lys 78, Ala 86, Lys 89, and His 90. The highly conserved CDGSH domain and the remarkable structural homology among proteins of the NEET family opens the question of whether a similar ligand binding site is present in CISD3. At variance with mitoNEET, which is homodimer, the two $[Fe_2S_2]$ cluster domains in CISD3 are not equivalent. Therefore, the ligand binding sites observed in mitoNEET correspond, in CISD3, to two different stretches: Val 41, Ala 42, Leu 43, Arg 64, Lys 66, Ser 74, Phe 77 Gln 78 for the N-terminal CDGSH domain and Thr 80, Gly 81, Leu 82, Ala 102, Gln 104, Thr 112, Ser 115 Glu 116, in the C-terminal CDGSH domain. As shown in Fig. 5, the electrostatic charge network of the two domains is different, with the C-term domain being apparently more similar to the situation occurring in mitoNEET with respect to the N-terminus potential binding site. This emphasizes the importance to extend the assignment and identify, as much as possible, residues around

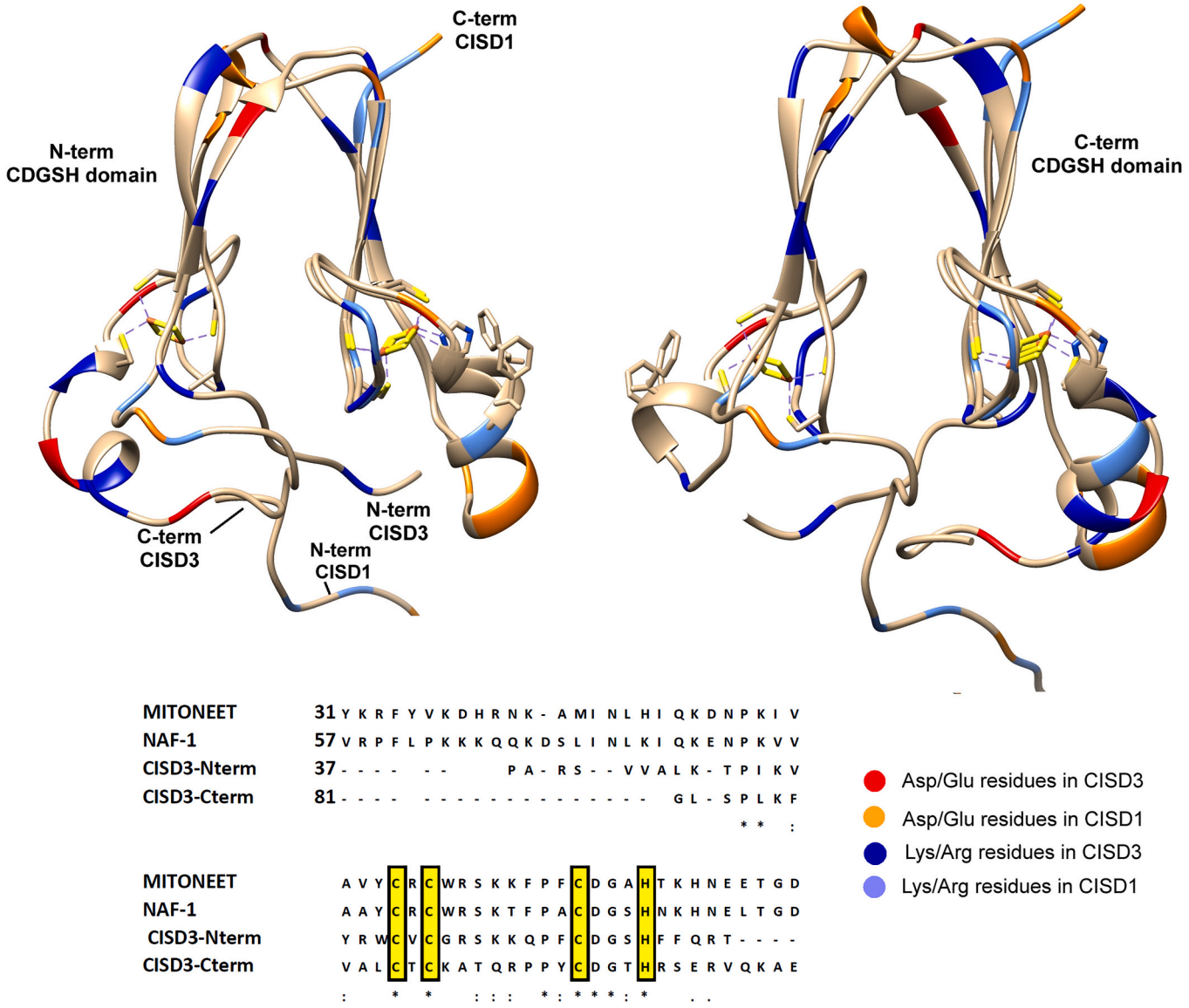

Fig. 5. Overlap between a single mitoNEET subunit and CISD3 crystal structure. On the left, mitoNEET was superimposed to the Nterm domain of CISD3, while on the right the overlap was with the CISD3 Cterm domain. Charged residues are highlighted. The primary sequence alignment is also shown. Overlaps were performed using the UCSF Chimera program; sequence alignment was obtained using Clustal W.

the clusters. Residues of the putative ligand binding site have a 4–12 Å distance range from the closest iron ion, therefore, the reduction of the blind sphere from 9 to 7 Å significantly improves the possibility to map the interaction in solution of CISD3 via HSQC experiments and chemical shift perturbations [43,50].

4. Conclusions

The role of CISD3 in mitochondrial functions and morphology is far from being elucidated [23–25]; it has been shown that CISD3 acts via molecular interactions that involve residues close to the FeS clusters [13,49,51–53]. Among the many different spectroscopic techniques able to investigate iron sulfur centers, NMR provides unique information at the atomic level in solution and therefore is capable to identify the residues involved in ligand binding. Here, we provide evidence that paramagnetic relaxation is a tool for signal assignment in the proximity of the cluster. Tailored experiments revive signals of the cluster environment, then relaxation rates provide an unambiguous and accurate information on the metal-proton distance which allows one to assign residues that do not have a complete network of scalar connectivities and to identify the key players of the biological function of paramagnetic metalloproteins.

5. Materials and methods

5.1. Protein expression and purification

The CISD3 gene Ala 37-Leu 127, preceded by a methionine and a glycine, was inserted into a pET28a(+) plasmid, resulting in a construct with 93 residues. The plasmid was used to transform *E. coli* BL21 (DE3) gold competent cells. Cell growth was performed in M9 (^{15}N, ^{13}C/^{15}N labelled) medium by adding 4 mL of Q solution and 500 μM Mohr's salt at 37 °C. When the culture reached an OD 600 of 0.8–1, 0.1 mM isopropyl β- d-1-thiogalactopyranoside (IPTG) was added to induce protein overexpression and the cells were incubated at 18 °C overnight. All the purification steps were performed in an anaerobic glovebox, as previously done for other FeS proteins [54]. Cells were resuspended in 80 mL of 20 mM Tris-HCl, 50 mM NaCl pH 7.5 degassed buffer, lysed by adding

CelLytic Reagent (0.8 g × 1 L culture) and incubating for 20 minutes. After incubation the lysate was diluted up to 200 mL, filtered using a 0.22 μm filter and then loaded in a HiTrap SP FF cationic exchange column. The column was washed with a step NaCl gradient, the NaCl concentration was increased in 50 mM increments, until CISD3 protein solution eluted with 20 mM Tris-HCl pH 7.5 and 300 mM NaCl. The purity of CISD3 sample was checked by SDS-PAGE gel (Fig. S6A). The final NMR sample had a protein concentration of 500 μM in 20 mM Tris-HCl, 300 mM NaCl, 2 mM dithiothreitol (DTT) pH 7.5 and 10% D_2O. The oxidation state of the protein was monitored via UV–Vis spectroscopy as shown in Fig. S6B.

5.2. NMR spectroscopy for backbone assignment and heteronuclear relaxation

Diamagnetic and paramagnetic experiments were recorded on CISD3 protein in its reduced 2$[Fe_2S_2]^+$ form. All NMR experiments used for resonance assignment were recorded on Bruker AVANCE 700 and 500 MHz spectrometers on 0.5 mM ^{13}C, ^{15}N-labelled samples in 50 mM phosphate buffer, 150 mM NaCl, pH 7.5, containing 10% (*v*/v) D_2O. All NMR spectra were collected at 298 K, processed using the standard Bruker software (Topspin 3.6) and analyzed through the CARA program [55]. The ^1H, ^{13}C, and ^{15}N resonance assignments were obtained through acquisition and analysis of diamagnetic and paramagnetic spectra. The complete battery of experiments used throughout this work is reported in Table S1. The FID data of the experiments reported in Table S1 have been deposited in BMRBig with the code: bmrbig82. ^{15}N longitudinal (R_1) and transverse (R_2) relaxation rates and {^1H}-^{15}N NOEs [56,57] were recorded at 298 K at 700 MHz, using a protein concentration of 0.3 mM. For {^1H}-^{15}N NOE measurements, delays of 5 s were used between repetitions of the pulse sequence. For ^{15}N- R_1 and ^{15}N -R_2 repetition delays of 3 s were used. For R_1 measurements, 10 experiments were recorded with delays of 10 ms, 40 ms, 80 ms, 125 ms, 200 ms, 400 ms, 650 ms, 900 ms, 1.5 s, 2.5 s. For R_2 measurements, 12 experiments were recorded with delays of 16.96 ms, 33.92 ms, 50.88 ms, 67.84 ms, 87.71 ms, 101.76 ms, 135.68 ms, 169.6 ms, 203.52 ms, 254.54 ms, 322.24 ms, 372.12 ms.

5.3. ^1H_N-relaxation experiments

Measurements of ^1H_N R_1 and R_2 relaxation rates, diamagnetic and paramagnetic, were carried out using 11.7 T Bruker AVANCE 500 equipped with a triple resonance, inverse detection, cryoprobe (TXI). ^1H_N relaxation measurements rates, both diamagnetic and paramagnetic, were recorded at 298 K at 500 MHz, using a protein concentration of 0.5 mM. The In-Phase (IP) experiments were acquired with acquisition and recycle delays of 56 ms and 2 s, respectively, and for the Anti-Phase (AP) experiments were 56 ms and 150 ms.

A series of thirteen ^1H_N R_1 ^{15}N-IR-HSQC-IP experiments were recorded using inversion recovery periods of 0.001 s, 0.01 s, 0.02 s, 0.05 s, 0.08 s, 0.12 s, 0.16 s, 0.2 s, 0.3 s, 0.5 s, 0.7 s, 1 s and 1.8 s. For each experiment, 32 scans were collected over 128 increments. A series of thirteen ^1H_N ^{15}N-IR-HSQC-AP experiments was recorded, using inversion recovery periods of 2 ms, 4 ms, 6 ms, 10 ms, 15 ms, 20 ms, 25 ms, 30 ms, 40 ms, 50 ms, 80 ms, 120 ms and 200 ms. For each experiment, 512 scans were collected over 128 increments. A series of sixteen ^1H_N R_2 ^{15}N-HSQC-IP experiments were recorded using transfer INEPT periods of 1.8 ms, 2.3 ms, 3 ms, 3.6 ms, 4.8 ms, 6 ms, 7.2 ms, 8.4 ms, 10.8 ms, 11.6 ms, 13.2 ms, 16 ms, 18 ms, 23.2 ms, 25.6 ms and 30.2 ms. For each experiment, 64 scans were collected over 156 increments. A series of twelve ^1H_N R_2-weighted ^{15}N-HSQC-AP experiments was recorded, using INEPT transfer periods of 0.1 ms, 0.2 ms, 0.3 ms, 0.6 ms, 0.7 ms, 1.0 ms, 1.2 ms, 1.6 ms, 2.0 ms, 2.8 ms, 4.0 ms, 5.0 ms. For each experiment, 768 scans were collected over 128 increments. Peaks were integrated using CARA software and data the different relaxation rates were calculated using EXCEL/ORIGIN software.

Abbreviations

CISD3	CDGSH iron-sulfur domain-containing protein 3
NMR	Nuclear Magnetic Resonance
HSQC	Heteronuclear Single Quantum Coherence

CRediT authorship contribution statement

Deborah Grifagni: Investigation, Visualization, Writing - original draft. **José M. Silva:** Investigation, Visualization, Writing - original draft. **Francesca Cantini:** Conceptualization, Visualization, Writing - review & editing. **Mario Piccioli:** Conceptualization, Supervision, Writing - review & editing. **Lucia Banci:** Conceptualization, Supervision, Writing - review & editing.

Declaration of Competing Interest

The authors declare that they have no known competing financial interests or personal relationships that could have appeared to influence the work reported in this paper.

Data availability

Data will be made available on request.

Acknowledgments

The authors acknowledge the support by the Italian Ministry for University and Research (Fondo Ordinario per gli Enti e le istituzioni di ricerca (FOE) funding) to the CERM/CIRMMP Italian Centre of Instruct-ERIC, a landmark ESFRI project. JMS acknowledges a Fellowship from TIMB3, grant no. 810856, funded by the Horizon 2020 research and innovation program of the European Commission. DG is a PhD student supported under the EOSC-Life Project (ID:824087) funded by the Horizon 2020 EC program.

Appendix A. Supplementary data

Supplementary data to this article can be found online at https://doi.org/10.1016/j.jinorgbio.2022.112089.

References

[1] Y. Lu, N. Yeung, N. Sieracki, N.M. Marshall, Nature 460 (2009) 855–862, https://doi.org/10.1038/nature08304.
[2] V. Laveglia, A. Giachetti, D. Sala, C. Andreini, A. Rosato, J. Chem. Inf. Model. vol. 62 (2022) 2951–2960, https://doi.org/10.1021/acs.jcim.2c00522. American Chemical Society.
[3] C. Spronk, S. Zerko, M. Gorka, W. Kozminski, B. Bardiaux, B. Zambelli, F. Musiani, M. Piccioli, P. Basak, F.C. Blum, R.C. Johnson, H. Hu, D.S. Merrell, M. Maroney, S. Ciurli, J. Biol. Inorg. Chem. 23 (2018) 1309–1330, https://doi.org/10.1007/s00775-018-1616-y.
[4] I.G. Bertini, E.I. Stiefel, G.S. Valentine, Biological Inorganic Chemistry: Structure and Reactivity, University Science Book, Sausalito CA, 2007.
[5] A. Warshel, P.K. Sharma, M. Kato, W.W. Parson, Biochim. Biophys. Acta 1764 (2006) 1647–1676, https://doi.org/10.1016/j.bbapap.2006.08.007.
[6] I.B. Trindade, A. Coelho, F. Cantini, M. Piccioli, R.O. Louro, J. Inorg. Biochem. 234 (2022), 111871, https://doi.org/10.1016/j.jinorgbio.2022.111871.
[7] F. Camponeschi, A. Gallo, M. Piccioli, L. Banci, Magnetic Reson. Discuss. 2 (2021) 203–211, https://doi.org/10.5194/mr-2021-2.
[8] T.E. Machonkin, W.M. Westler, J.L. Markley, J. Am. Chem. Soc. 126 (2004) 5413–5426, https://doi.org/10.1021/ja037077i.
[9] I.B. Trindade, M. Invernici, F. Cantini, R.O. Louro, M. Piccioli, FEBS J. 288 (2021) 3010–3023, https://doi.org/10.1111/febs.15615.
[10] L. Banci, I. Bertini, V. Calderone, S. Ciofi-Baffoni, A. Giachetti, D. Jaiswal, M. Mikolajczyk, M. Piccioli, J. Winkelmann, Proc. Natl. Acad. Sci. U. S. A. 110 (2013) 7136–7141, https://doi.org/10.1073/pnas.1302378110.
[11] I.B. Trindade, M. Invernici, F. Cantini, R.O. Louro, M. Piccioli, Inorg. Chim. Acta 514 (2021), 119984, https://doi.org/10.1016/j.ica.2020.119984.

[12] R. Mittler, M. Darash-Yahana, Y.S. Sohn, F. Bai, L. Song, I.Z. Cabantchik, P. A. Jennings, J.N. Onuchic, R. Nechushtai, Antioxid. Redox Signal. 30 (2019) 1083–1095, https://doi.org/10.1089/ars.2018.7502.
[13] I. Ferecatu, S. Goncalves, M.P. Golinelli-Cohen, M. Clemancey, A. Martelli, S. Riquier, E. Guittet, J.M. Latour, H. Puccio, J.C. Drapier, E. Lescop, C. Bouton, J. Biol. Chem. 289 (2014) 28070–28086, https://doi.org/10.1074/jbc.M114.548438.
[14] C. Mons, T. Botzanowski, A. Nikolaev, P. Hellwig, S. Cianferani, E. Lescop, C. Bouton, M.P. Golinelli-Cohen, Biochemistry 57 (2018) 5616–5628, https://doi.org/10.1021/acs.biochem.8b00777.
[15] T. Takahashi, M. Yamamoto, K. Amikura, K. Kato, T. Serizawa, K. Serizawa, D. Akazawa, T. Aoki, K. Kawai, E. Ogasawara, J. Hayashi, K. Nakada, M. Kainoh, J. Pharmacol. Exp. Ther. 352 (2015) 338–345, https://doi.org/10.1124/jpet.114.220673.
[16] G. Song, F. Tian, H. Liu, G. Li, P. Zheng, J. Phys. Chem. Lett. 12 (2021) 3860–3867, https://doi.org/10.1021/acs.jpclett.0c03852.
[17] O. Karmi, H.B. Marjault, L. Pesce, P. Carloni, J.N. Onuchic, P.A. Jennings, R. Mittler, R. Nechushtai, J. Biol. Inorg. Chem. 23 (2018) 599–612, https://doi.org/10.1007/s00775-018-1538-8.
[18] M.L. Paddock, S.E. Wiley, H.L. Axelrod, A.E. Cohen, M. Roy, E.C. Abresch, D. Capraro, A.N. Murphy, R. Nechushtai, J.E. Dixon, P.A. Jennings, Proc. Natl. Acad. Sci. U. S. A. 104 (2007) 14342–14347, https://doi.org/10.1073/pnas.0707189104.
[19] F. Camponeschi, M. Piccioli, L. Banci, Molecules 27 (2022) 8218, 10.3390/molecules27238218.
[20] C.H. Lipper, O. Karmi, Y.S. Sohn, M. Darash-Yahana, H. Lammert, L. Song, A. Liu, R. Mittler, R. Nechushtai, J.N. Onuchic, P.A. Jennings, Proc. Natl. Acad. Sci. U. S. A. 115 (2018) 272–277, https://doi.org/10.1073/pnas.1715842115.
[21] S. Sengupta, R. Nechushtai, P.A. Jennings, J.N. Onuchic, P.A. Padilla, R.K. Azad, R. Mittler, Sci. Rep. 8 (2018) 4840, https://doi.org/10.1038/s41598-018-23305-6.
[22] O. Karmi, H.B. Marjault, F. Bai, S. Roy, Y.S. Sohn, M. Darash Yahana, F. Morcos, K. Ioannidis, Y. Nahmias, P.A. Jennings, R. Mittler, J.N. Onuchic, R. Nechushtai, Proc. Natl. Acad. Sci. U. S. A. 119 (2022), e2121491119, https://doi.org/10.1073/pnas.2121491119.
[23] S.D. King, C.F. Gray, L. Song, R. Mittler, P.A. Padilla, PLoS One 16 (2021), e0245174, https://doi.org/10.1371/journal.pone.0245174.
[24] Y. Li, X. Wang, Z. Huang, Y. Zhou, J. Xia, W. Hu, X. Wang, J. Du, X. Tong, Y. Wang, Cell Death Dis. 12 (2021) 839, https://doi.org/10.1038/s41419-021-04128-2.
[25] M.P. Golinelli-Cohen, E. Lescop, C. Mons, S. Goncalves, M. Clemancey, J. Santolini, E. Guittet, G. Blondin, J.M. Latour, C. Bouton, J. Biol. Chem. 291 (2016) 7583–7593, https://doi.org/10.1074/jbc.M115.711218.
[26] S. Ciofi-Baffoni, A. Gallo, R. Muzzioli, M. Piccioli, J. Biomol. NMR 58 (2014) 123–128, https://doi.org/10.1007/s10858-013-9810-2.
[27] M. Invernici, I.B. Trindade, F. Cantini, R.O. Louro, M. Piccioli, J. Biomol. NMR 74 (2020) 431–442, https://doi.org/10.1007/s10858-020-00334-w.
[28] M. Piccioli, Magnetochemistry 6 (2020) 46, https://doi.org/10.3390/magnetochemistry6040046.
[29] F. Camponeschi, R. Muzzioli, S. Ciofi-Baffoni, M. Piccioli, L. Banci, J. Mol. Biol. 431 (2019) 4514–4522, https://doi.org/10.1016/j.jmb.2019.08.018.
[30] I. Solomon, Phys. Rev. 99 (1955) 559–565, https://doi.org/10.1103/PhysRev.99.559.
[31] B.A. Lyons, M. Tashiro, L. Cedergren, B. Nilsson, G.T. Montelione, Biochemistry 32 (1993) 7839–7845, https://doi.org/10.1021/bi00082a001.
[32] S. Shimotakahara, C.B. Rios, J.H. Laity, D.E. Zimmerman, H.A. Scheraga, G. T. Montelione, Biochemistry 36 (1997) 6915–6929, https://doi.org/10.1021/bi963024k.
[33] J. Iwahara, C. Tang, G. Marius Clore, J. Magn. Reson. 184 (2007) 185–195, https://doi.org/10.1016/j.jmr.2006.10.003.
[34] I. Bertini, M.M. Couture, A. Donaire, L.D. Eltis, I.C. Felli, C. Luchinat, M. Piccioli, A. Rosato, Eur. J. Biochem. 241 (1996) 440–452, https://doi.org/10.1111/j.1432-1033.1996.00440.x.
[35] J.L. Battiste, G. Wagner, Biochemistry 39 (2000) 5355–5365, https://doi.org/10.1021/bi000060h.
[36] L.W. Donaldson, N.R. Skrynnikov, W.Y. Choy, D.R. Muhandiram, B. Sarkar, J. D. Forman-Kay, L.E. Kay, J. Am. Chem. Soc. 123 (2001) 9843–9847, https://doi.org/10.1021/ja011241p.
[37] C. Tang, J. Iwahara, G.M. Clore, Nature 444 (2006) 383–386, https://doi.org/10.1038/nature05201.
[38] A.N. Volkov, J.A.R. Worrall, E. Holtzmann, M. Ubbink, Proc. Natl. Acad. Sci. U. S. A. 103 (2006) 18945–18950, https://doi.org/10.1073/pnas.0603551103.
[39] C. Tang, C.D. Schwieters, G.M. Clore, Nature 449 (2007) 1078–1082, https://doi.org/10.1038/nature06232.
[40] M. John, G. Pintacuda, A.Y. Park, N.E. Dixon, G. Otting, J. Am. Chem. Soc. 128 (2006) 12910–12916, https://doi.org/10.1021/ja063584z.
[41] Q. Miao, C. Nitsche, H. Orton, M. Overhand, G. Otting, M. Ubbink, Chem. Rev. 122 (2022) 9571–9642, https://doi.org/10.1021/acs.chemrev.1c00708.
[42] I. Bertini, B. Jimenez, M. Piccioli, J. Magn. Reson. 174 (2005) 125–132, https://doi.org/10.1016/j.jmr.2005.01.014.
[43] D. Brancaccio, A. Gallo, M. Piccioli, E. Novellino, S. Ciofi-Baffoni, L. Banci, J. Am. Chem. Soc. 139 (2017) 719–730, https://doi.org/10.1021/jacs.6b09567.
[44] I.B. Trindade, G. Hernandez, E. Lebegue, F. Barriere, T. Cordeiro, M. Piccioli, R. O. Louro, J. Biol. Inorg. Chem. 26 (2021) 313–326, https://doi.org/10.1007/s00775-021-01854-y.
[45] J.A. Zuris, Y. Harir, A.R. Conlan, M. Shvartsman, D. Michaeli, S. Tamir, M. L. Paddock, J.N. Onuchic, R. Mittler, Z.I. Cabantchik, P.A. Jennings, R. Nechushtai, Proc. Natl. Acad. Sci. U. S. A. 108 (2011) 13047–13052, https://doi.org/10.1073/pnas.1109986108.
[46] H.B. Marjault, O. Karmi, K. Zuo, D. Michaeli, Y. Eisenberg-Domovich, G. Rossetti, B. de Chassey, J. Vonderscher, I. Cabantchik, P. Carloni, R. Mittler, O. Livnah, E. Meldrum, R. Nechushtai, Commun. Biol. 5 (2022) 437, https://doi.org/10.1038/s42003-022-03393-x.
[47] Y. Wang, A.P. Landry, H. Ding, J. Biol. Chem. 292 (2017) 10061–10067, https://doi.org/10.1074/jbc.M117.789800.
[48] O. Karmi, S.H. Holt, L. Song, S. Tamir, Y. Luo, F. Bai, A. Adenwalla, M. Darash-Yahana, Y.S. Sohn, P.A. Jennings, R.K. Azad, J.N. Onuchic, F. Morcos, R. Nechushtai, R. Mittler, PLoS One 12 (2017), e0175796, https://doi.org/10.1371/journal.pone.0175796.
[49] R.M. Bieganski, M.L. Yarmush, J. Mol. Graph. Model. 29 (2011) 965–973, https://doi.org/10.1016/j.jmgm.2011.04.001.
[50] F. Camponeschi, N.R. Prusty, S.A.E. Heider, S. Ciofi-Baffoni, L. Banci, J. Am. Chem. Soc. 142 (2020) 10794–10805, https://doi.org/10.1021/jacs.0c02266.
[51] Y. Wang, J. Lee, H. Ding, Nitric Oxide Biol. Chem. 89 (2019) 96–103, https://doi.org/10.1016/j.niox.2019.05.007.
[52] W.J. Geldenhuys, R. Skolik, M.E. Konkle, M.A. Menze, T.E. Long, A.R. Robart, Bioorg. Med. Chem. Lett. 29 (2019) 901–904, https://doi.org/10.1016/j.bmcl.2019.01.041.
[53] Z. Cheng, A.P. Landry, Y. Wang, H. Ding, J. Biol. Chem. 292 (2017) 3146–3153, https://doi.org/10.1074/jbc.M116.766774.
[54] V. Maione, D. Grifagni, F. Torricella, F. Cantini, L. Banci, J. Biol. Inorg. Chem. 25 (2020) 501–508, https://doi.org/10.1007/s00775-020-01778-z.
[55] M. Invernici, G. Selvolini, J.M. Silva, G. Marrazza, S. Ciofi-Baffoni, M. Piccioli, Chem. Commun. (Camb.) 58 (2022) 3533–3536, https://doi.org/10.1039/d1cc03566e.
[56] N.A. Farrow, R. Muhandiram, A.U. Singer, S.M. Pascal, C.M. Kay, G. Gish, S. E. Shoelson, T. Pawson, J.D. Forman-Kay, L.E. Kay, Biochemistry 33 (1994) 5984–6003, https://doi.org/10.1021/bi00185a040.
[57] S. Grzesiek, A. Bax, J. Am. Chem. Soc. 115 (1993) 12593–12594, https://doi.org/10.1021/ja00079a052.